J Nanostruct 14(4): 1197-1210, Autumn 2024

RESEARCH PAPER

Amelioration and Characterization the Structural and Optical Properties of Polyvinyl Alcohol (PVA)/ Polyaniline (PANI)/ Copper Oxide (Cu_2O) Nanocomposites

Hassan Sarab Kimar *, Sameer Hassan Hadi Al-nesrawy

Department of Physics, College of Education for Pure Sciences, University of Babylon, Babylon, Iraq

ARTICLE INFO

Article History:
Received 09 July 2024
Accepted 26 September 2024
Published 01 October 2024

Keywords:
Cu_2O NPs
FESEM
FTIR
OM
Optical Characteristic
PVA/PANI

ABSTRACT

This study covers how to solution cast polyvinyl alcohol (PVA)/ polyaniline (PANI) composites reinforced with 0, 2, 4, 6 and 8 wt.% copper oxide (Cu_2O). The samples underwent characterization using OM (Optical Microscopy), FESEM (Field Emission Scanning Electron Microscopy), FTIR (Fourier Transform Infrared Spectroscopy), and UV-Vis (Ultraviolet-Visible) analytical procedures. The OM pictures revealed the formation of network routes inside the polymeric matrix as charge carriers, which increased with higher concentrations of nanoparticles. The nanocomposite surface was analyzed using a field emission scanning electron microscope (FESEM). FESEM revealed the consistent dispersion of Cu_2O nanoparticles in (PVA/PANI) matrix polymers. The application of Fourier transformation spectroscopy (FTIR) allowed for the detection and analysis of molecular vibrations inside the structure of the nanocomposite. The FTIR measurement demonstrated polymer matrix- Cu_2O nanoparticle interaction. The Cu_2O nanoparticles and PVA/PANI polymers matrix exhibit physical interaction as observed in FTIR investigations. A thorough analysis was conducted on the optical characteristics. Elevating the concentration of Cu_2O nanoparticles in PVA/PANI sheets resulted in higher absorbance and lower transmittance. The integration of (Cu_2O) nanoparticles at a concentration of 8 wt.% in the (PVA/PANI/ Cu_2O) nanocomposite resulted in a decrease in the energy gap. More precisely, the energy gap reduced from 4.6 electron volts (eV) to 3.2 eV for the permissible indirect transition, and from 4.47 eV to 2.9 eV for the impermissible indirect transition. The weight percentages of Cu_2O nanoparticles have a positive correlation with their absorption coefficient, extinction coefficient, refractive index, real and imaginary parts of dielectric constants, and optical conductivity. The results support the excellent optical capabilities of PVA/PANI/ Cu_2O film nanocomposites, thereby promoting their use in photodetector applications.

How to cite this article
Kimar H., Al-esrawy S. Amelioration and Characterization the Structural and Optical Properties of Polyvinyl Alcohol (PVA)/ Polyaniline (PANI)/ Copper Oxide (Cu_2O) Nanocomposites. J Nanostruct, 2024; 14(4):1197-1210. DOI: 10.22052/JNS.2024.04.020

INTRODUCTION

The utilization of polymer nanocomposites has garnered significant interest in the academic community due to its exceptional efficacy and varied attributes, achieved by incorporating a limited quantity of nanoparticles into the polymer matrix. Introducing nano-scale fillers into polymer nanocomposites has been discovered to greatly

---

* *Corresponding Author Email: hasansgumar.92@gmail.com*

enhance their characteristics, even at lower concentrations in comparison to conventional polymer composites [1, 2]. The chemical and physical characteristics of inorganic nanoparticles (NPs) and their electrostatic interactions with polymeric chains have an impact on the molecular structure and microstructure [3]. Regulating nanocomposite materials can be accomplished by modifying the concentration of their constituent components within the polymeric matrix composition [4,5]. Composite materials have been widely used in many industries such as sensors, aviation, optics, and electronics. However, these devices consistently necessitate supplementary features and functionalities. Nanocomposites comprising organic and inorganic materials provide the collective benefits of organic polymers and inorganic chemicals, leading to a diverse array of applications [6-10].

Nanofillers were incorporated into a host matrix using polyvinyl alcohol (PVA) as the base material. Polyvinyl alcohol (PVA) is esteemed for its remarkable characteristics, such as its low density of 1.36 g/cm^3, high melting point of 230 °C, and its effortless solubility in water. These attributes render it suitable for utilization as a framework for charge storage components and for providing robust insulation in numerous applications [11]. Polyvinyl alcohol (PVA) is added to the solar cells because of its elongated carbon chain that contains hydroxyl groups, which facilitate the formation of hydrogen bonds. Polymer nanocomposites allow for the convenient evaluation of modifications in the band gap and complex band structure of both amorphous and semi-crystalline materials [12]. Incorporating metal oxides, such as zinc, copper, magnesium, and cerium oxides, into polymers can significantly modify their structural, optical, and electrical characteristics [13].

Nanostructures made of conducting polymers, including PANI and polypyrrole, along with their composites at the nanoscale, have become a promising field of research with the capacity to produce novel materials for advanced technologies. The nano-dimensional metal oxide/polymer composites demonstrate superior electrical and magnetic properties when compared to the original metal oxide and conductive polymers. Moreover, these composites exhibit remarkable durability in various environments, including air, chemical, and electrical conditions, as demonstrated by transistors (field effect). Moreover, the production process is uncomplicated [14]. The main electrically charged particles in PANI are mainly polarons and bipolarons, which are made stable by the presence of counter ions incorporated into the polymer during its manufacture. Conductive polymers have recently attracted considerable attention in the field of organic electronics because of their potential usefulness in several energy conversion devices, such as photovoltaic and solar cells, biosensors, and others [15].

Polyaniline (PANI) is extensively researched as a conducting polymer due to its easy production, affordable synthesis, and excellent resistance to environmental and thermal changes. PANI can be readily synthesized using either chemical or electrochemical methods using acidic aqueous solutions [16].

Cuprous oxide (Cu_2O) is an abundant p-type semiconductor that is naturally present in the Earth's crust and is not harmful to living organisms. The material exhibits a high absorption coefficient that covers the violet to green areas of the solar spectrum. This feature enables it to effectively transform solar energy into either electrical or chemical energy [17]. Cu2O is considered a highly coveted inorganic system with a wide range of applications in gas detection, CO oxidation, photocatalysis, photochemical synthesis of H2 from water, and generation of photocurrent [18]. Cu2O nanoparticles can be synthesized using many techniques such as electrodeposition, chemical synthesis, thermal relaxation, liquid-phase reduction, vacuum evaporation, and green synthesis [19].

The purpose of this study is to investigate the structural and optical properties of (PVA/PANI/Cu_2O) nanocomposites.

MATERIALS AND METHOD

A solution was prepared by dissolving 0.9 g of polyvinyl alcohol (PVA) polymer in 50 mL of distilled water. In order to dissolve the substance completely, a magnetic stirrer was used to vigorously mix the liquid at a temperature of 70 ^{o}C for a period of 30 minutes or until complete dissolution was achieved, resulting in the production of a uniform mixture. After cooling the solution to 40 ^{o}C, it was added 0.1 g of polyaniline (PANI) was added to synthesis the polymer blend. The work entailed integrating Cu_2O nanoparticles into a PVA/PANI solution at concentrations of 2, 4, 6 and 8 wt.%, with the aim of producing nanocomposites. Drying afterwards, the casting procedure was utilized.

The Bruker Vertex-70, a device produced in Germany, was employed for the purpose of conducting Fourier Transform Infrared Spectroscopy (FTIR). An optical microscope supplied by Olympus named (Top View) type (Nikon 73346) with an automatically controlled camera under a (10x) magnification was employed to define the films' surface. Analyzed using a

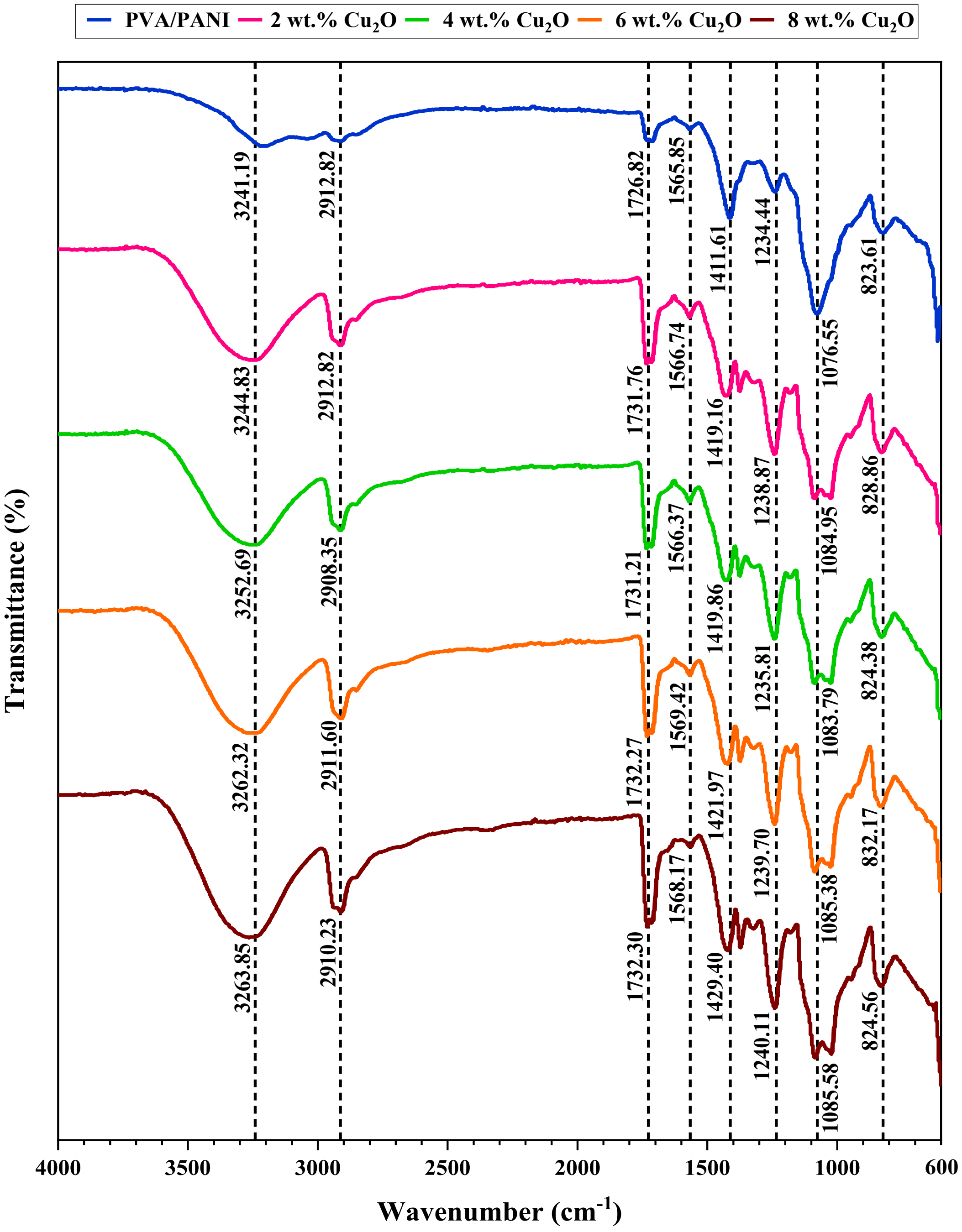

Fig. 1. The FTIR of PVA/PANI/Cu$_2$O nanocomposites: (a) of (PVA/PANI), (b) of 2 wt.% Cu$_2$O, (c) of 4wt.% Cu$_2$O, (d) of 6 wt.% Cu$_2$O and e) of 8 wt.% Cu$_2$O

Hitachi SU6600 variable pressure system equipped field emission scanning electron microscope (FESEM), the structural features of (PVA/PANI/Cu_2O) nanocomposites were examined. The gadget covered the spectral region from 500 to 4000 cm^{-1}. The optical analysis of the PVA/PANI/Cu_2O nanocomposite was conducted using a UV-18000A-Shimadzu spectrophotometer.

The absorption coefficient (α) is given as [20]:

$$\alpha = 2.303 * A/t \tag{1}$$

Where t: thickness of the samples, A: represent the optical absorbance. The optical indirect energy gap is given by [21]:

$$(\alpha h v)^{1/m} = B\,(hv - E_g) \tag{2}$$

Where, B is constant, hυ is the photon energy, Eg is the energy gap, m = 2 and 3 to indirect transition of allowed and forbidden. The index of refractive (n) is defined by [22]

$$n = (1 + R^{\frac{1}{2}})/(1 - R^{\frac{1}{2}}) \tag{3}$$

Which R is the reflection, the coefficient of extinction (k) is determined by [23]

$$k = \frac{\alpha\lambda}{4\pi} \tag{4}$$

Where λ is the wavelength. The dielectric constant parts: real (ε_1), and imaginary (ε_2) are given by [24].

$$\varepsilon_1 = n^2 - k^2 \tag{5}$$

$$\varepsilon_2 = 2nk \tag{6}$$

The optical conductivity (σ_{op}) is defined by[24]

$$\sigma_{opt.} = \frac{\alpha n c}{4\pi} \tag{7}$$

Where c is velocity of light.

RESULT AND DISCUSSION

The vibration and rotation of molecular groups in a substance are revealed by FTIR spectra. The FTIR spectra of (PVAPANI/Cu_2O) nanocomposites in the wave number range (500-4000) cm^{-1} are shown in Fig. 1. In image (a), FTIR spectra of pure (PVA/PANI) polymers are reveals absorption band at 3241.19 cm^{-1} corresponding to N–H stretching vibrations of secondary amine of PANI and the band 2912.82 cm^{-1} attributed to the asymmetric stretching of CH_2 [25]. The peaks at 1726.82 cm^{-1} proved the existence of (C-O) stretching aldehyde. Two peaks at 1565.85 and 1411.61 cm^{-1} are recognized to CH_2 and vibrations of (CH + OH) groups of PVA [26]. The peak at 1234.44 cm^{-1} is attributed to the stretching of the C–N+• polaron structure, which represents the electrically conductive state of doped PANI. The peak detected at 1076.55 cm^{-1} can be ascribed to the rotational movement of robust C-O-C bending vibrations. The presence of the C–Cl stretching peak at 823.61 cm^{-1} in the band peak confirms the incorporation of chlorine (Cl-) in the produced polyaniline films using hydrochloric acid (HCl) [27].

The spectra of PVA/PANI with varying concentrations of Cu_2O NPs are shown in pictures b, c, d and e. According to these images, the addition of Cu_2O NPs induced a shift in some bands and a change in some intensities. According to the FTIR research, introducing varying concentrations of (Cu_2O) in images b, c, d and e results in the displacement of some of the bonds but not the development of new peaks. As a result, no contact occurs between the (Cu_2O) nanoparticle and the PVA/PANI polymer matrix. This result are deal with researchers [28].

The optical microscope allows for the observation of changes in the surface morphology of PVA/PANI/Cu_2O nanocomposites. Fig. 2 displays the optical microscope (OM) images of PVA/PANI/ Cu_2O nanocomposites at a magnification of 10x for all samples. The surface picture of the polymer mix film (a) displays a uniform phase without any phase segregation. Furthermore, it exhibits an enhanced shape and a sleek surface, showing the successful polymer ratio of PVA/PANI. The image (b-e) clearly demonstrates the uniform distribution of Cu_2O nanoparticles on the surface of the PVA/PANI polymer films. This effect gets more noticeable as the weight fraction of Cu_2O increases. The nanocomposite has a nearly circular configuration consisting of particles that are uniformly uniform in shape. This is because nanoparticles (NPs) possess a substantial surface area, and the polymeric solution, which comprises diverse polar groups, exhibits a pronounced affinity towards Cu_2O. Consequently, the nanoparticles arrange themselves in the polymer chain, leading to a denser Cu_2O structure. As a result, the texture of the material is improved. This process provided a suitable method for creating nanocomposite films [29].

The placement of copper oxide nanoparticles

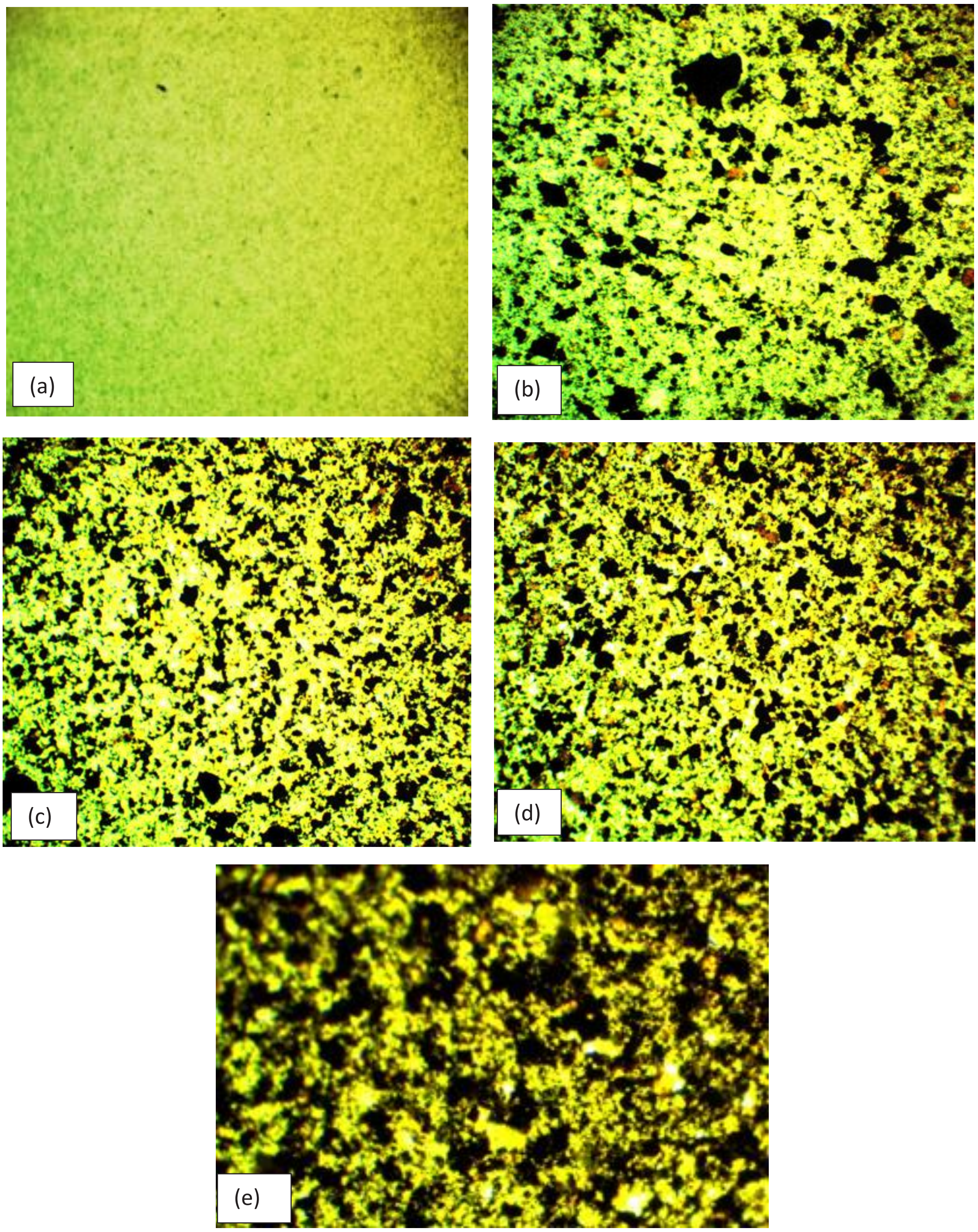

Fig. 2. The optical microscope of PVA/PANI/Cu_2O nanocomposites: (a) of (PVA/PANI), (b) of 2 wt.% Cu_2O, (c) of 4wt.% Cu_2O, (d) of 6 wt.% Cu_2O and e) of 8 wt.% Cu_2O

(Cu_2O NPs) within the polymer is analyzed using a field emission scanning electron microscope (FESEM), and the influence of these particles on the nanocomposites is then verified. Films produced from (PVA/PANI/Cu_2O) nanocomposites with varied Cu_2O nanoparticle concentrations are depicted in FESEM images in Fig. 3. It is clear from image (a) that the polymer is cohesive

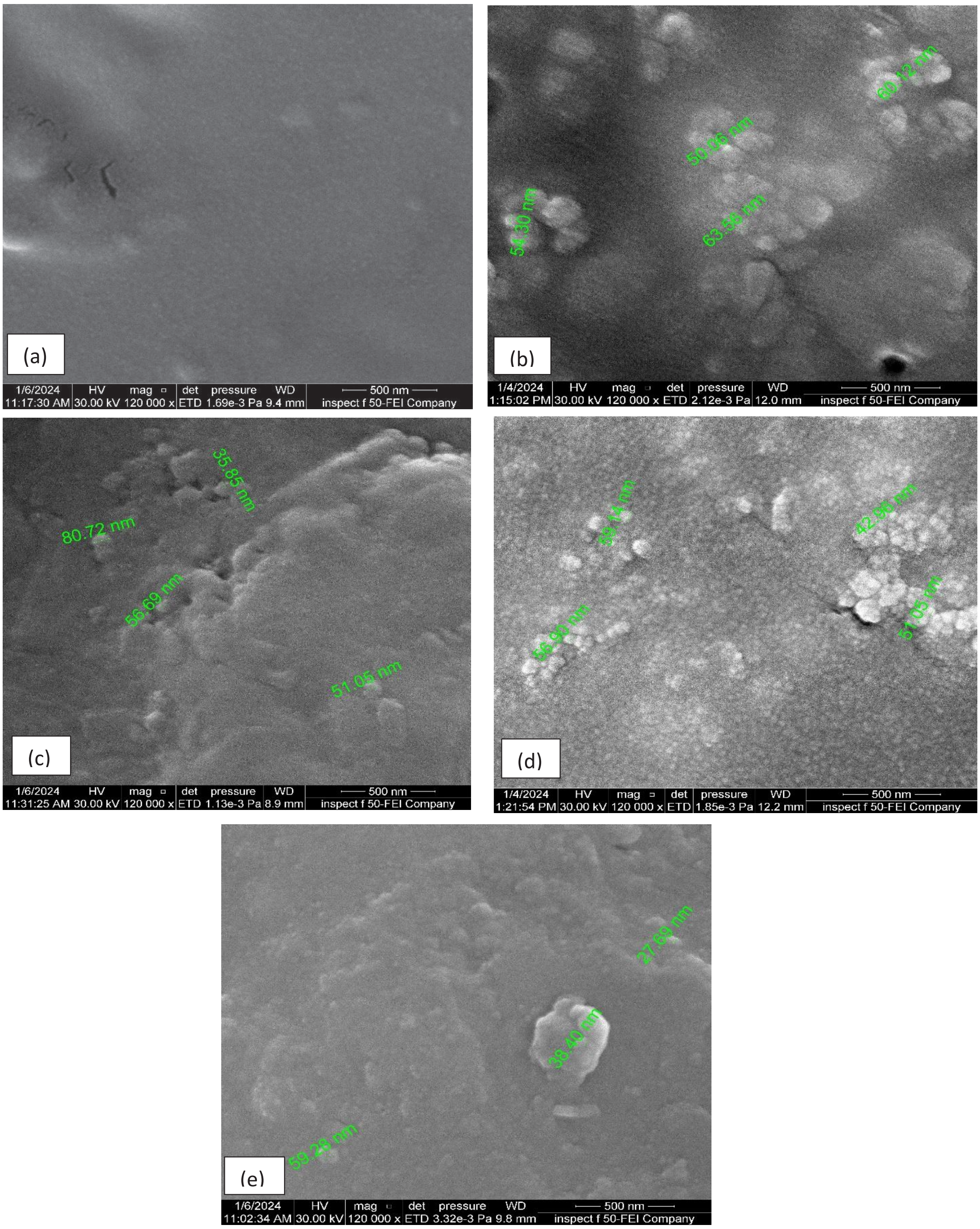

Fig. 3. The FESEM of PVA/PANI/Cu_2O nanocomposites: (a) of (PVA/PANI), (b) of 2 wt.% Cu_2O, (c) of 4wt.% Cu_2O, (d) of 6 wt.% Cu_2O and e) of 8 wt.% Cu_2O

and homogenous, and that adding more Cu_2O nanoparticles to (PVA/PANI) polymer changes the surface structure of the system (see images b, c, d and e). The average grain size as measured from FESEM images was 73, 56, 46 and 42 nm for 2, 4, 6 and 8% for Cu_2O NPs respectively. One concludes from the FESEM images that the average grain size decreased with the increment of Cu_2O NPs. This outcome aligns with the findings of researchers [30].

Fig. 4 depicts the absorbance spectra of the produced compound. The measurements were performed in the wavelength range of 200-1100 nm. Distinct peaks at 440 nm are found, illustrating the π- π* transition of PANI. This transition is attributed to the benzenoid ring and is related to the degree of coupling between surrounding phenylene rings in the polymeric chains. This impact is caused by the accumulation of the system. Consequently, there is an increased level of interconnectedness among the components, leading to a reduction in the energy gap between the valence band and the conduction band. The improved electrical conductivity of the nanocomposites can be attributed to the transition of the π* benzenoid ring and the creation of the polaron band. The considerable fall in intensity recorded at approximately 220 nm could potentially be related to the n−π* transition. The figure illustrates a correlation between the quantity of Cu_2O and a reduction in the intensity of absorption peaks. This shows that the addition of Cu_2O nanoparticles as a filler in the polyaniline and polyvinyl alcohol matrix has an impact on the absorption spectra of the nanocomposites being generated. This outcome refers to researchers [31].

The Fig. 5 illustrates the transmission properties of the PVA/PANI/Cu_2O nanocomposite at different content of Cu_2O loading. The figure illustrates a drop in transmittance as the ratio of Cu_2O increases. The increase in surface roughness can be attributed to the aggregation of nanoparticles. As a result, the dispersion of light is amplified because of the intensified surface fragmentation. Despite the possible cost repercussions, the nanocomposite films display reduced transmission of UV wavelengths, making them suitable for use in pharmaceutical packaging due to this induced property of absorption [32].

The absorption coefficient is given from the relation 1. Fig. 6 depicts the absorbance coefficient of PVA/PANI and a nanocomposite of PVA/PANI and copper oxide (Cu_2O) with different ratios of Cu_2O loading. Based on the results depicted in the figure, it is evident that the absorption coefficient of all samples shows a proportional rise with an increase in NPs. This indicates an increase in the transport of electric charge within the nanocomposites. The absorption coefficients

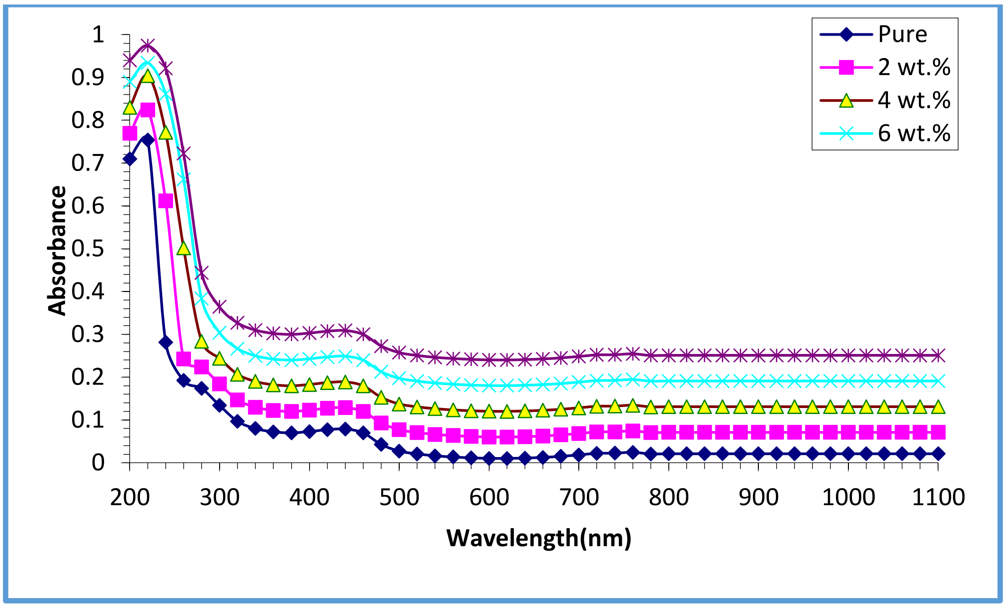

Fig. 4. Absorbance spectra of PVA/PANI/Cu_2O nanocomposites

of all prepared samples demonstrate low values at low energies, suggesting a restricted probability of electron transport. Nevertheless, these coefficients exhibit an upward trend when the energy of the input photon escalates, signifying an augmented likelihood of electron transfer. This indicates that the incident photons have enough energy to successfully interact with the atoms. The

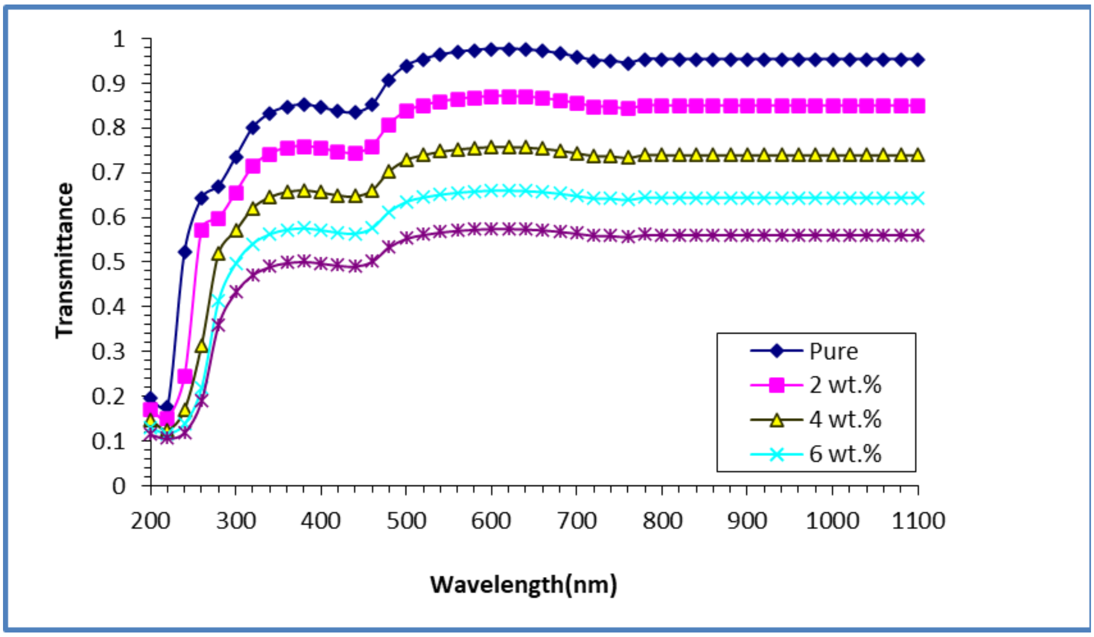

Fig. 5. Transmittance spectra of PVA/PANI/Cu_2O nanocomposites

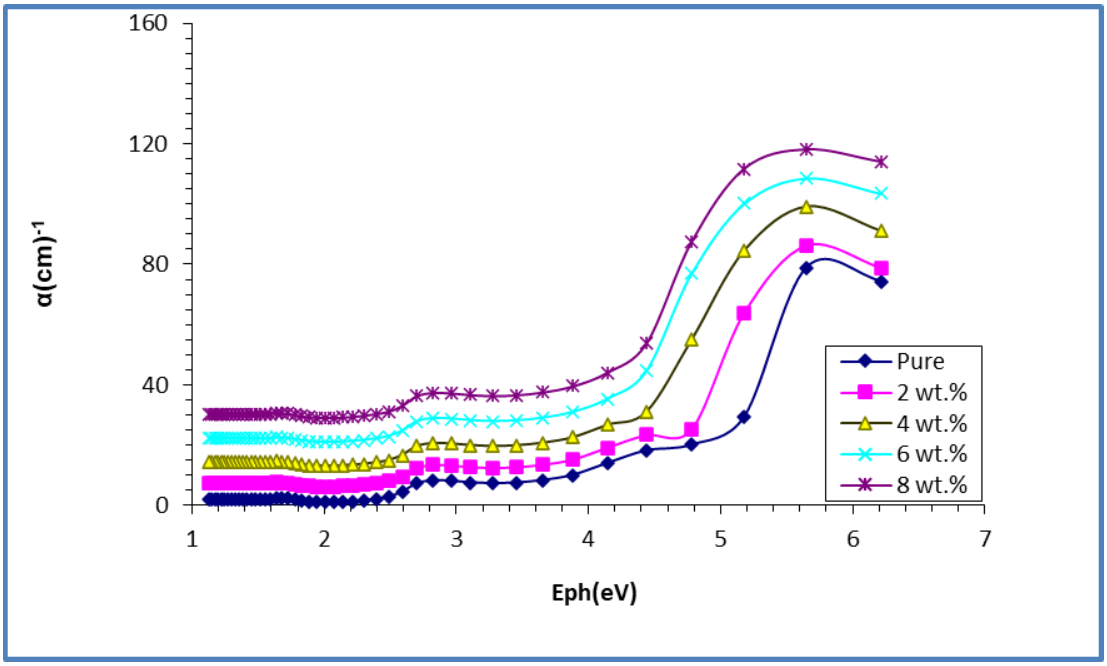

Fig. 6. Absorption coefficient of PVA/PANI/Cu_2O nanocomposites

measured α values of the generated films, which are less than 10^4 cm^{-1}, indicate a strong likelihood of indirect electronic transitions taking place. These results are consistent [33].

The energy gap is given by the relation 2. Figs. 7 and 8 illustrate the indirect band gap of both pure PVA/PANI and PVA/PANI/Cu_2O nanocomposite. Utilizing the intercept of the expanded linear segment. A linear segment was generated by isolating a section of the depicted curve in Figs. 4 and 5 to analyze the disparity in energy. The graphic illustrates a notable decrease in the energy disparity as the concentration of Cu_2O NPs increases. In PVA/PANI/Cu_2O nanocomposites, the allowed energy gap between the valence band and the conduction band drops from 4.6 eV in PVA/PANI polymers to 3.2 eV. The observed energy difference between the valence band and the conduction band, referred to as the forbidden band gap, dropped from 4.47 eV for PVA/PANI to 2.9 eV for the PVA/PANI/Cu_2O nanocomposites. The decrease in value was a result of modifying the proportion of the polymer and raising the load ratio from 0 to 8 wt.%. The observed behavior can be attributed to the oscillations in localized levels of parity and delivery packages. The organization of connectivity package tiers corresponds to the findings derived from various scholarly investigations. Table 1 demonstrates the value of the allowed and forbidden energy gaps. This result is agreed upon by researchers [39].

The extinction coefficient (k) is determined by relation 4. Fig. 9 depicts the extinction coefficient (k) of PVA/PANI/Cu_2O nanocomposites. Fig. 8

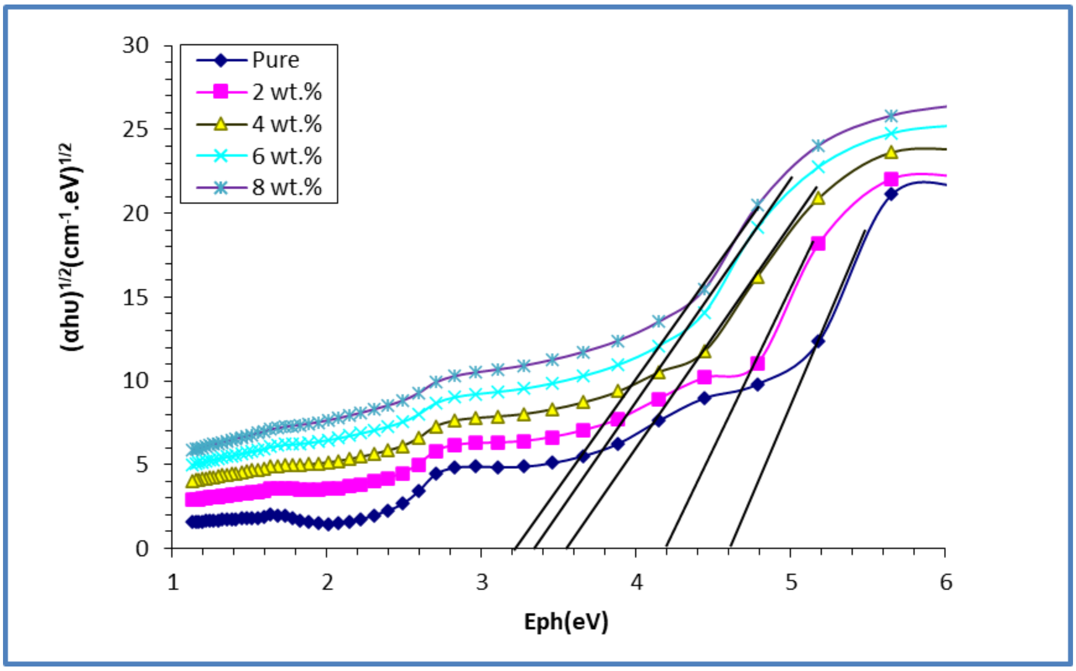

Fig. 7. Relation between $(\alpha h\upsilon)^{1/2}$ versus ($h\upsilon$) for PVA/PANI/Cu_2O nanocomposites

Table 1. Values for the allowed and forbidden energy gap of PVA/PANI/Cu_2O nanocomposites

wt.% of Cu_2O	Allowed Eg (eV)	Forbidden Eg (eV)
0	4.6	4.47
2	4.2	4.08
4	3.46	3.3
6	3.36	3.02
8	3.2	2.9

shows that the extinction coefficient of PVA/PANI/Cu_2O nanocomposites increases as the wavelength increases. This behavior may be attributed to the concurrent rise in photon energy.

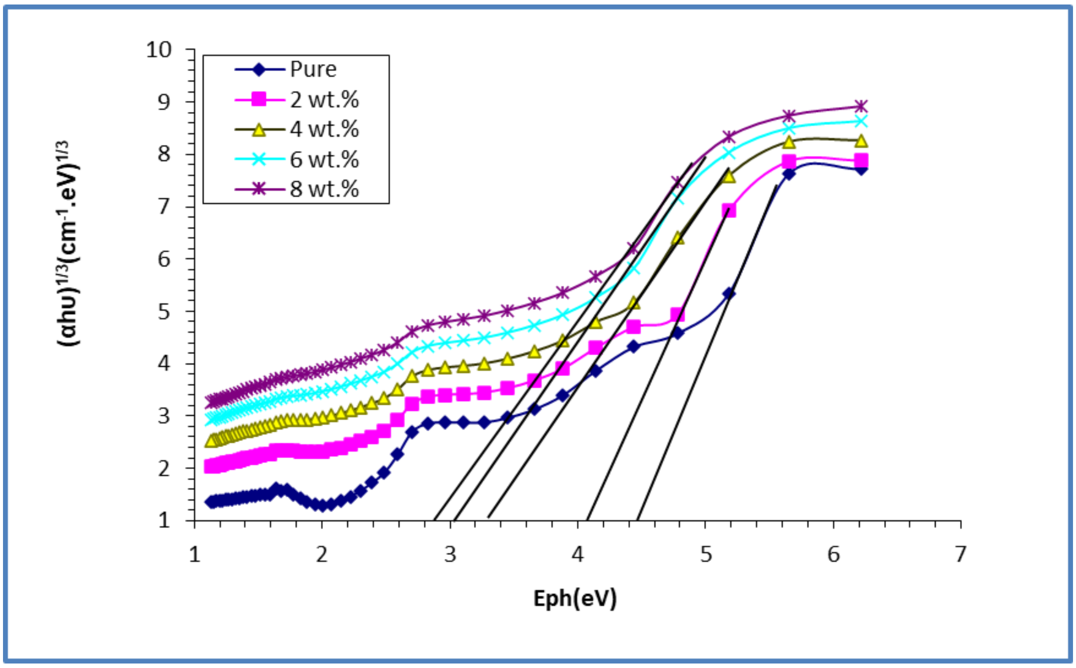

Fig. 8. Relation between $(\alpha h\upsilon)^{1/3}$ versus $(h\upsilon)$ for PVA/PANI/Cu_2O nanocomposites

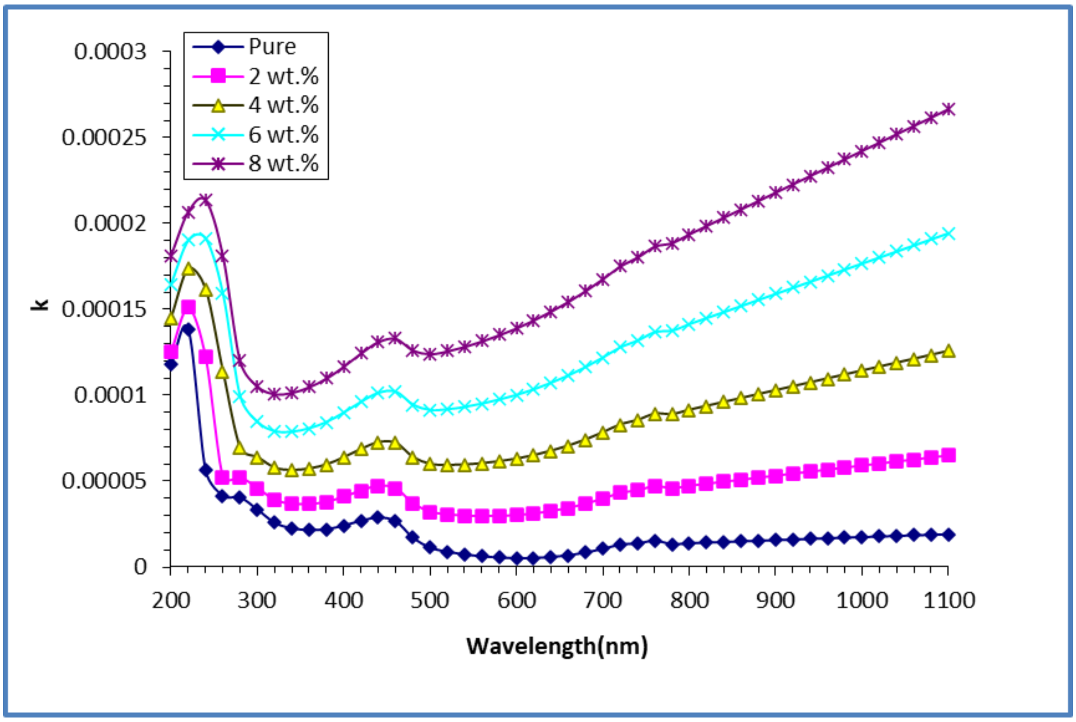

Fig. 9. Extinction coefficient of PVA/PANI/Cu_2O nanocomposites.

The correlation between the concentration ratio of Cu_2O nanoparticles and the extinction coefficient of nanocomposites is readily apparent. This phenomenon can be explained by an increase in the absorption of incoming light [34].

The refractive index (n) is determined by relation 3. Fig. 9 illustrates the refractive index (n) of PVA/PANI/Cu_2O nanocomposites. Fig. 10

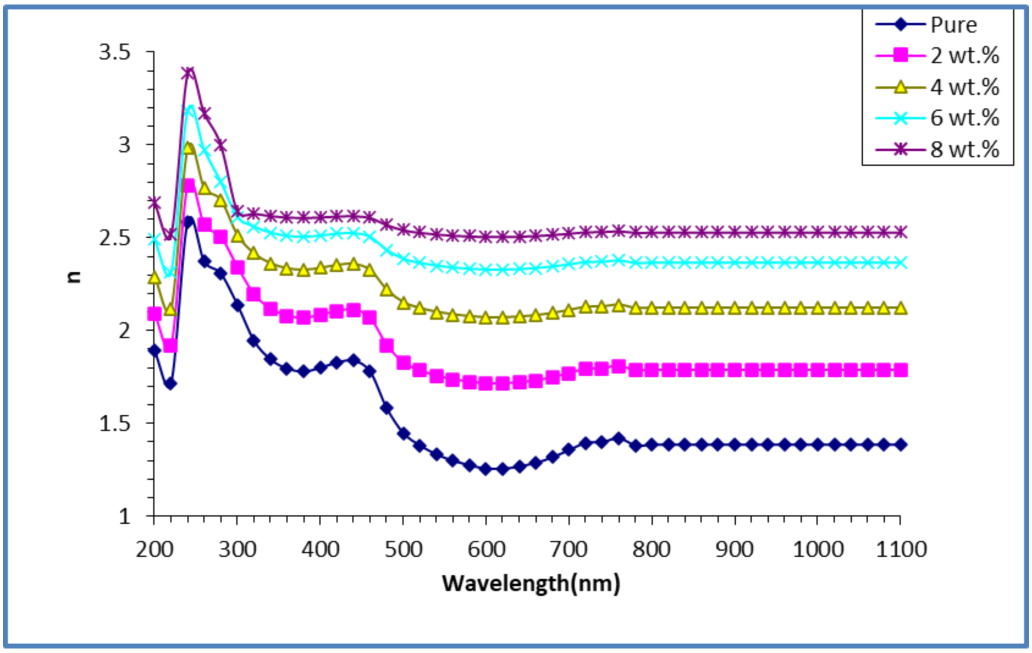

Fig. 10. Refractive index of PVA/PANI/Cu_2O nanocomposites

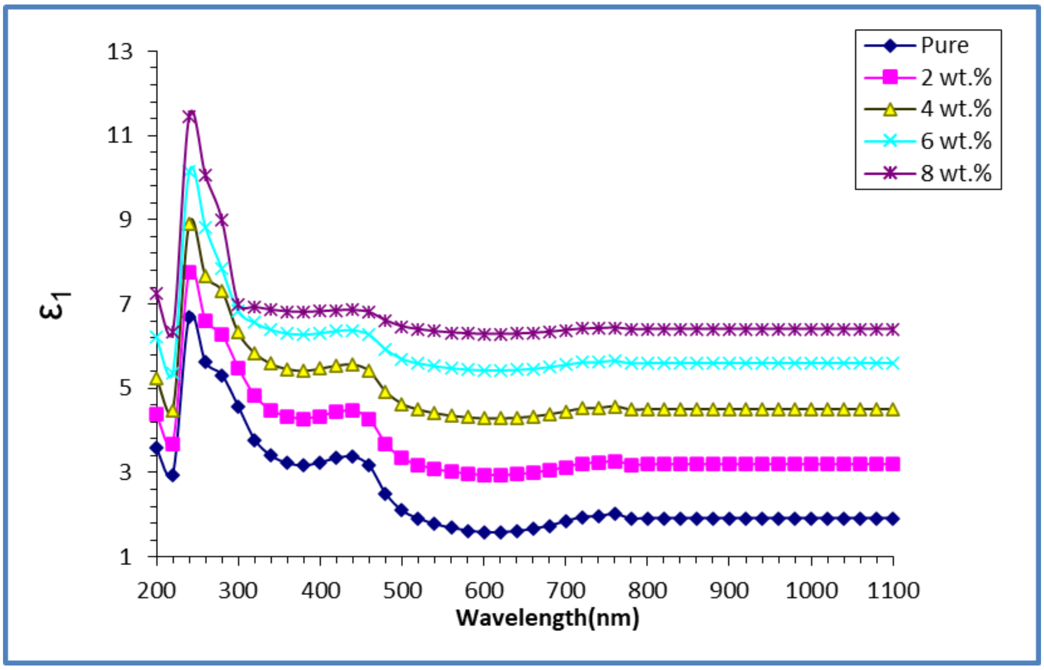

Fig. 11. Real dielectric constant of PVA/PANI/Cu_2O nanocomposites

demonstrates that the index of refraction for PVA/PANI/Cu$_2$O nanocomposites has a prominent peak at lower energies, specifically at 300 nm, and then decreases at higher energies. The refractive index remains constant in the visible and near-infrared (NIR) spectrum. Furthermore, it has

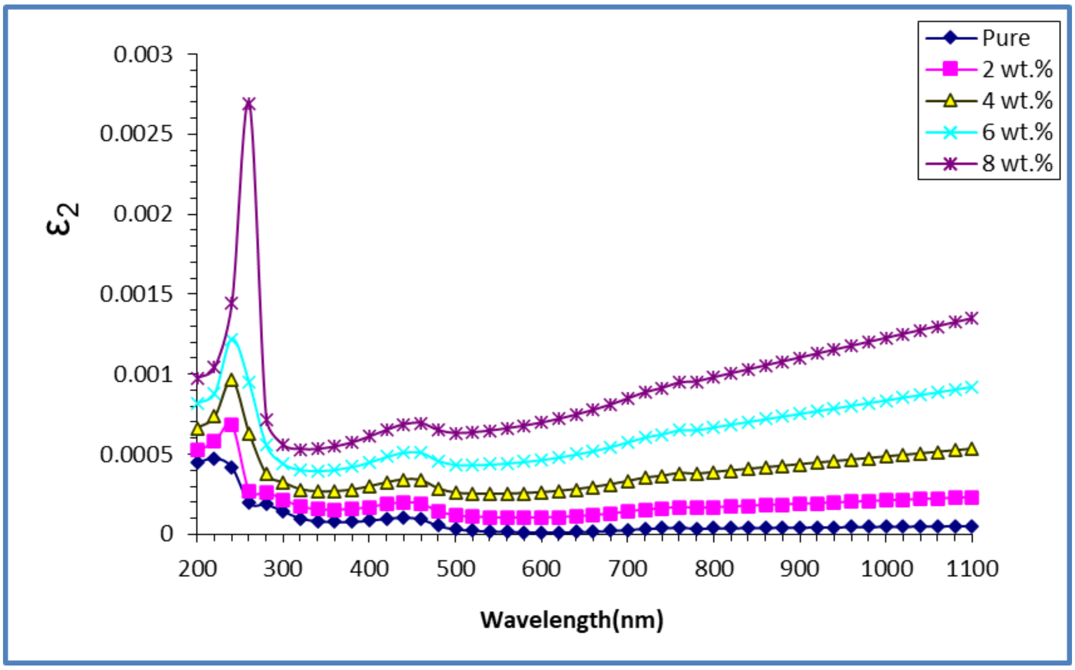

Fig. 12. Imaginary dielectric constant of PVA/PANI/Cu$_2$O nanocomposites

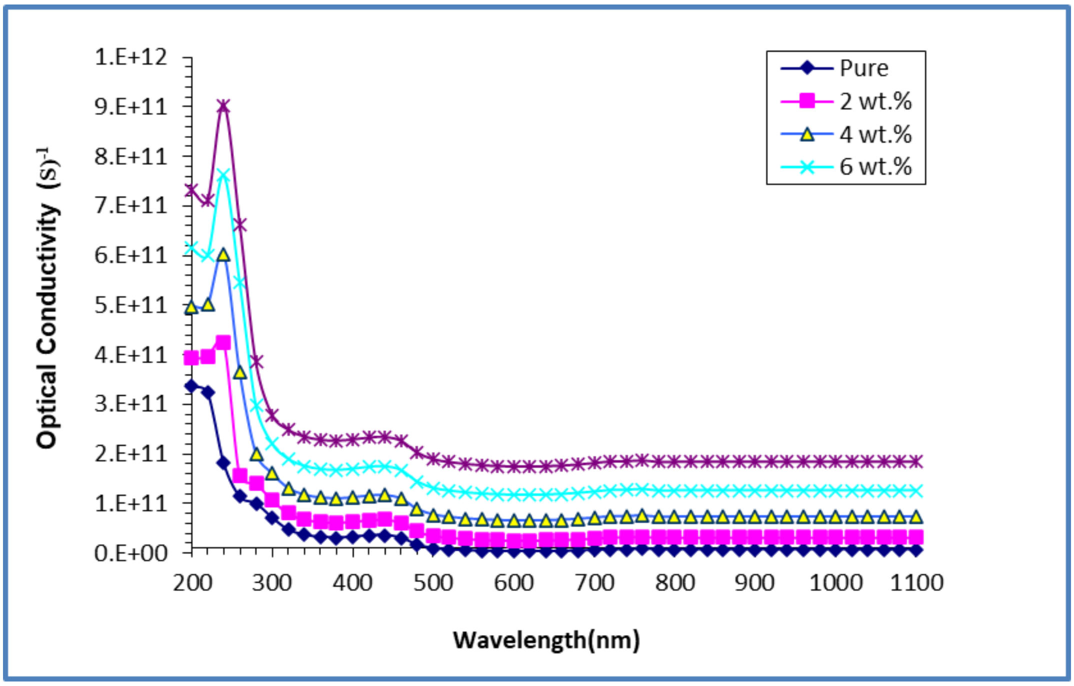

Fig. 13. Optical conductivity of PVA/PANI/Cu$_2$O nanocomposites

been noted that the refractive index rises when the concentration ratio of Cu$_2$O nanoparticles (NPs) increases. This behavior can be ascribed to the concurrent augmentation of nanocomposite density [35].

The dielectric constant is composed of two parts: the real part (ε_1) and the imaginary part (ε_2) are given in equation 5, 6. Figs. 11 and 12 depict the fluctuations found in the real component (ε_1) and imaginary component (ε_2) of the dielectric constant for pure PVA/PANI and a nanocomposite of PVA/PANI/Cu$_2$O with varying proportions of Cu$_2$O nanoparticles (NPs). The data presented indicates that the dielectric constant of pure PVA/PANI polymer and PVA/PANI/Cu$_2$O nanocomposites has greater values for both the real and imaginary components at shorter wavelengths, and diminishes as the wavelength increases. The nanocomposite films display a prominent increase in both the real and imaginary values as the wavelength decreases. This is followed by a substantial decrease in higher energy levels. The observed resemblance can be elucidated by the fact that the effective dielectric constant is predominantly influenced by the magnitudes of (n) rather than (k), considering that the latter values are considerably less than the refractive index, particularly when squared [36].

The optical conductivity (σ_{op}) is definite by relation 7. Fig. 13 depicts the optical conductivity of the pure PVA/PANI polymers and the PVA/PANI/Cu$_2$O nanocomposite, with varying concentrations of Cu$_2$O NPs. The pure PVA/PANI polymers and PVA/PANI/Cu$_2$O nanocomposites demonstrates a notable enhancement in optical conductivity at shorter wavelengths, followed by a reduction at longer wavelengths. This behavior can be explained by the concurrent increase in the absorption coefficient. The relationship between the concentration of Cu$_2$O nanoparticles and the observed optical conductivity is found to be directly proportional. The observed phenomena can be ascribed to the rise in the absorption coefficient [37].

CONCLUSION

This work presents a brief summary of a highly effective casting method used in the production of PVA/PANI/Cu$_2$O nanocomposites. The optical microscope (OM) images revealed the formation of network routes within the polymeric matrix as charge carriers, as the concentrations of nanoparticles increased. The dispersion of Cu$_2$O NPs within the PVA/PANI polymers matrix was validated by FESEM. The FTIR analysis has demonstrated the existence of tangible interactions between the PVA/PANI polymer matrix and Cu$_2$O NPs. The results indicate a direct relationship between the amount of Cu$_2$O nanoparticles and the absorbance of the PVA/PANI/Cu2O nanocomposite, leading to a decrease in transmittance. The addition of Cu$_2$O nanoparticles to the PVA/PANI polymers at a concentration of 8 weight percent led to a decrease in their energy gap. The presence of Cu$_2$O NPs is directly correlated with many optical properties, including as optical conductivity, absorption coefficient, extinction coefficient, refractive index, and the real and imaginary components of dielectric constants. Consequently, based on this outcome, it can be inferred that the PVA/PANI/Cu$_2$O nanocomposite is suitable for utilization in photodetector applications.

CONFLICT OF INTEREST

The authors declare that there is no conflict of interests regarding the publication of this manuscript.

REFERENCES

1. Varshney PK, Gupta S. Natural polymer-based electrolytes for electrochemical devices: a review. Ionics. 2011;17(6):479-483.
2. Atta MR, Alsulami QA, Asnag GM, Rajeh A. Enhanced optical, morphological, dielectric, and conductivity properties of gold nanoparticles doped with PVA/CMC blend as an application in organoelectronic devices. Journal of Materials Science: Materials in Electronics. 2021;32(8):10443-10457.
3. Morsi MA, Rajeh A, Al-Muntaser AA. Reinforcement of the optical, thermal and electrical properties of PEO based on MWCNTs/Au hybrid fillers: Nanodielectric materials for organoelectronic devices. Composites Part B: Engineering. 2019;173:106957.
4. Cha J, Kim J, Ryu S, Hong SH. Comparison to mechanical properties of epoxy nanocomposites reinforced by functionalized carbon nanotubes and graphene nanoplatelets. Composites Part B: Engineering. 2019;162:283-288.
5. Choudhary S. Characterization of amorphous silica nanofiller effect on the structural, morphological, optical, thermal, dielectric and electrical properties of PVA–PVP blend based polymer nanocomposites for their flexible nanodielectric applications. Journal of Materials Science: Materials in Electronics. 2018;29(12):10517-10534.
6. Mohammed MK, Al-Nafiey A, Al-Dahash G. Manufacturing Graphene and Graphene-based Nanocomposite for Piezoelectric Pressure Sensor Application: A Review. Nano Biomed Eng. 2021;13(1).
7. Mohammed MK, Abdullah EH, Hassan D, Hashim A. Effect of Titanium Nitrate Nanoparticles on Optical Properties of PVA/PEG Blend for Optoelectronics Detectors. Revue des

composites et des matériaux avancés. 2022;32(6):305-309.
8. Ahmed H, Hashim A. Fabrication of PVA/NiO/SiC Nanocomposites and Studying their Dielectric Properties For Antibacterial Applications. Egyptian Journal of Chemistry. 2019;0(0):0-0.
9. Kadhim K, Agool I, Hashim A. Synthesis of (PVA-PEG-PVP-TiO_2) Nanocomposites for Antibacterial Application. Materials Focus. 2016;5(5):436-439.
10. Hassan ES, Qader KY, Hadi EH, Chiad SS, Habubi NF, Abass KH. Sensitivity of Nanostructured Mn-Doped Cobalt Oxide Films for Gas Sensor Application. Nano Biomed Eng. 2020;12(3).
11. Hayder N, Hashim A, Habeeb MA, Rabee BH, Hadi AG, Mohammed MK. Analysis of Dielectric Properties of PVA/ PEG/In_2O_3 Nanostructures for Electronics Devices. Revue des composites et des matériaux avancés. 2022;32(5):261-264.
12. Mohammed AJ, Al-nesrawy SH. Nano Ferrite Incorporated Poly (Vinyl Pyrrolidone (PVP) /Poly (Vinyl Alcohol (PVA) Blend: Preparation and Investigation of Structural, Morphological and Optical Properties. Neuroquantology. 2022;20(4):251-258.
13. Widodo S, Krsitiantoro T. Synthesis of Zinc Oxide (ZnO) Nano Particles Using Sol Gel Method as Active Material on Gas Sensor. Advances in Physics Research: Atlantis Press; 2014.
14. Rahman Khan MM, Wee YK, Mahmood WAK. Effects of CuO on the morphology and conducting properties of PANI nanofibers. Synthetic Metals. 2012;162(13-14):1065-1072.
15. Linganathan P, Sundararajan J, Samuel JM. Synthesis, Characterization, and Photoconductivity Studies on Poly(2-chloroaniline) and Poly(2-chloroaniline)/CuO Nanocomposites. Journal of Composites. 2014;2014:1-9.
16. Toman MS, Al-nesrawy SH. New Fabrication (PVA-CMC -PbO) Nanocomposites Structural and Electrical Properties. Neuroquantology. 2021;19(4):38-46.
17. Bali 2017 International Conference Proceeding IPCET-17, CM3E-17, ABEMS-17, ICEEE-17, ICCEE-17, ICASE-17, ICAFE-17, EBHRM-17, LHHSS-17 and LEBHM-172017 2017/10/11: EIRAI.
18. Mohammed MA. Structural, Optical, Electrical and Gas Sensor Properties of ZrO2 Thin Films prepared by Sol-Gel Technique. Neuroquantology. 2020;18(3):22-27.
19. Topnani N, Kushwaha S, Athar T. Wet Synthesis of Copper Oxide Nanopowder. International Journal of Green Nanotechnology: Materials Science and Engineering. 2009;1(2):M67-M73.
20. Jothibas M, Manoharan C, Johnson Jeyakumar S, Praveen P. Study on structural and optical behaviors of In_2O_3 nanocrystals as potential candidate for optoelectronic devices. Journal of Materials Science: Materials in Electronics. 2015;26(12):9600-9606.
21. Abdel-Baset T, Elzayat M, Mahrous S. Characterization and Optical and Dielectric Properties of Polyvinyl Chloride/Silica Nanocomposites Films. International Journal of Polymer Science. 2016;2016:1-13.
22. Agarwal S, Saraswat YK, Saraswat VK. Study of Optical Constants of ZnO Dispersed PC/PMMA Blend Nanocomposites. Open Physics Journal. 2016;3(1):63-72.
23. Standards. Archives and Museum Informatics. 1990;4(2):23-24.
24. Tyagi C, Devi A. Alteration of structural, optical and electrical properties of CdSe incorporated polyvinyl pyrrolidone nanocomposite for memory devices. Journal of Advanced Dielectrics. 2018;08(03):1850020.
25. Sydulu Singu B, Srinivasan P, Pabba S. Benzoyl Peroxide Oxidation Route to Nano Form Polyaniline Salt Containing Dual Dopants for Pseudocapacitor. Journal of The Electrochemical Society. 2011;159(1):A6-A13.
26. Zeng X-R, Ko T-M. Structures and properties of chemically reduced polyanilines. Polymer. 1998;39(5):1187-1195.
27. Hussain AMP, Kumar A. Electrochemical synthesis and characterization of chloride doped polyaniline. Bull Mater Sci. 2003;26(3):329-334.
28. Al-Khafaji RSA. Synthesis of Blend Polymer (PVA / PANI)/ Copper (1) Oxide Nanocomposite: Thermal Analysis and UV-Vis Spectra Specifications. Iraqi Journal of Science. 2021:3888-3900.
29. Babu JR, Ravindhranath K, Kumar KV. Structural and Electrical Properties of Sodium Citrate Doped Poly(vinyl alcohol) Films for Electrochemical Cell Applications. Asian J Chem. 2017;29(5):1049-1055.
30. Yang M-Z, Dai C-L, Lin W-Y. Fabrication and characterization of polyaniline/PVA humidity microsensors. Sensors (Basel, Switzerland). 2011;11(8):8143-8151.
31. Trchová M, Šeděnková I, Morávková Z, Stejskal J. Conducting polymer and ionic liquid: Improved thermal stability of the material – A spectroscopic study. Polymer Degradation and Stability. 2014;109:27-32.
32. Ali RS, Mohammed MK, Khadayeir AA, Abood ZM, Habubi NF, Chiad SS. Structural and Optical Characterization of Sprayed nanostructured Indium Doped Fe_2O_3 Thin Films. Journal of Physics: Conference Series. 2020;1664(1):012016.
33. Damoom MM, Saeed A, Alshammari EM, Alhawsawi AM, Yassin AY, Abdulwahed JAM, et al. The role of TiO2 nanoparticles in enhancing the structural, optical, and electrical properties of PVA/PVP/CMC ternary polymer blend: nanocomposites for capacitive energy storage. Journal of Sol-Gel Science and Technology. 2023;108(3):742-755.
34. Rajeswari N, Selvasekarapandian S, Karthikeyan S, Prabu M, Hirankumar G, Nithya H, et al. Conductivity and dielectric properties of polyvinyl alcohol–polyvinylpyrrolidone poly blend film using non-aqueous medium. J Non-Cryst Solids. 2011;357(22-23):3751-3756.
35. Mireles LK, Wu M-R, Saadeh N, Yahia LH, Sacher E. Physicochemical Characterization of Polyvinyl Pyrrolidone: A Tale of Two Polyvinyl Pyrrolidones. ACS omega. 2020;5(47):30461-30467.
36. Habeeb MA, Rahdi WH. Retraction Note: Titanium carbide nanoparticles filled PVA-PAAm nanocomposites: structural and electrical characteristics for application in energy storage. Optical and Quantum Electronics. 2024;56(11).
37. Soliman TS, Vshivkov SA, Elkalashy SI. Structural, thermal, and linear optical properties of SiO_2 nanoparticles dispersed in polyvinyl alcohol nanocomposite films. Polymer Composites. 2020;41(8):3340-3350.